

Triplet Superconducting Correlations in Oxide Heterostructures with a Composite Ferromagnetic Interlayer

G. A. Ovsyannikov^{a, b, *}, A. E. Sheyerman^{a, c}, A. V. Shadrin^{a, b}, Yu. V. Kislinskii^a,
K. Y. Constantinian^a, and A. Kalabukhov^b

^a Kotel'nikov Institute of Radio Engineering and Electronics, Russian Academy of Sciences,
ul. Mokhovaya 11-7, Moscow, 125009 Russia

* e-mail: gena@hitech.cplire.ru

^b Department of Microtechnology and Nanoscience, Chalmers University of Technology, S-41296 Gothenburg, Sweden

^c Moscow Institute of Physics and Technology (State University),
Institutskii per. 9, Dolgoprudnyi, Moscow region, 141700 Russia

Received December 29, 2012

The superconducting current induced by the penetration of the long-range triplet component of superconducting correlations into a composite ferromagnetic interlayer has been detected in mesa-heterostructures based on oxide cuprate superconductors $\text{YBa}_2\text{Cu}_3\text{O}_{7-\delta}$ and Au/Nb bilayer films with the composite oxide interlayer that is made of ferromagnetic films of manganite $\text{La}_{0.7}\text{Sr}_{0.3}\text{MnO}_3$ and ruthenate SrRuO_3 and has a thickness much larger than the length of correlations determined by the exchange field. The deviation of the superconducting current in the mesa-heterostructure with the fraction of the second harmonic of 13% from a sinusoidal current–phase relation has been detected; this deviation can also be due to the generation of the triplet component of superconducting correlations in the ferromagnet.

DOI: 10.1134/S0021364013030089

It is known that long-range triplet superconducting correlations can occur in a nonuniformly magnetized ferromagnet (F) between two singlet superconductors (S) [1, 2]. The triplet pairing was previously considered for the explanation of the appearance of the A phase in superfluid ^3He [3]. In SFS structures with uniform magnetization, the projection of the spin of a superconducting pair on the direction of the magnetization is conserved and singlet and triplet superconducting correlations with zero spin projection appear in F [2, 4]; they penetrate into F and oscillate in it with the characteristic length ξ_F determined by the magnetic exchange energy E_{ex} . In particular, in the dirty limit, $\xi_F = \sqrt{(\hbar D/E_{\text{ex}})}$, where $D = v_F l/3$ is the diffusion coefficient, v_F is the Fermi velocity, and l is the mean free path. In the case of the generation of long-range triplet superconducting correlations with non-zero (± 1) spin projection, the exchange interaction does not suppress superconductivity [2] and the length of correlations (e.g., in the dirty limit) is determined by the temperature T as $\xi_N = \sqrt{(\hbar D/k_B T)}$ as for SNS contacts with normal metal (N). Since the condition $k_B T \ll E_{\text{ex}}$ is usually satisfied in experiments, the appearance of long-range triplet superconducting correlations in a ferromagnet leads to the anomalously strong proximity effect and the existence of the superconducting current in SFS structures at sufficiently large distances between superconductors.

The first experimental indications of the anomalously strong proximity effect explained by the generation of long-range triplet superconducting correlations in a ferromagnet were obtained when studying an Andreev interferometer with a holmium film bridge having spiral magnetization [5] and SFS structures with CrO_2 , which is a semimetallic ferromagnet with 100% polarization [6, 7]. These experimental data were confirmed when studying single-crystal cobalt nanowires [8] and SFS structures with Heusler alloy [9], and a ferromagnet with spiral magnetization [10] and “synthetic” interlayers consisting of alternating PdNi and Ho layers [11]. The authors of [12] recently reported a change in the superconducting critical temperature of the SFF' structure consisting of a superconducting film S deposited on the bilayer structure of ferromagnets with noncollinear magnetization [12].

At the same time, the investigations of long-range triplet superconducting correlations in SFS structures with a manganite ferromagnetic interlayer with 100% polarization, where singlet superconducting correlations cannot appear, give contradictory results. On one hand, the authors of [13, 14] reported the effect of long-range triplet superconducting correlations on Andreev reflection in structures with a $\text{La}_{0.7}\text{Ca}_{0.3}\text{MnO}_3$ manganite; on the other hand, superconducting current was not observed in them except for the case of pinholes [15, 16].

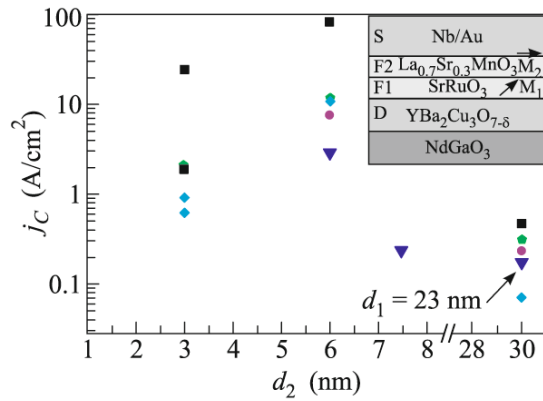


Fig. 1. Superconducting current density in the mesa-heterostructure versus the thickness of the LSMO film d_2 at $T = 4.2$ K. The thickness of the SRO film d_1 varied in the range of 4–5 nm. The squares, circles, pentagons, triangles, and diamonds mark junctions with the sizes in the plane of the substrate of 10×10 , 20×20 , 30×30 , 40×40 , and 50×50 μm , respectively. The data for the mesa-heterostructure with the thickness of the SRO layer $d_1 = 23$ nm are shown separately. The inset shows the cross section of the hybrid heterostructure with the composite interlayer. The arrows schematically show the directions of the magnetization vectors.

In this work, we experimentally study hybrid heterostructures $S/M/S_d$ (where S is the Nb/Au bilayer structure and S_d is the $\text{YBa}_2\text{Cu}_3\text{O}_x$ cuprate superconductor) with a composite magnetic oxide interlayer M consisting of two thin layers of $\text{La}_{0.7}\text{Ca}_{0.3}\text{MnO}_3$ and SrRuO_3 ferromagnets with noncollinear magnetization directions. Such structures were theoretically considered in [17–20].

Mesa-heterostructures square with the in-plane side L from 10 to 50 μm were fabricated on (110) NdGaO_3 substrates [21]. The lower electrode was an epitaxial film of $\text{YBa}_2\text{Cu}_3\text{O}_{7-\delta}$ cuprate superconductor and the upper superconducting electrode was a Nb/Au bilayer structure. The interlayer M con-

sisted of two ferromagnets: F_1 was SrRuO_3 (SRO) and F_2 was $\text{La}_{0.7}\text{Sr}_{0.3}\text{MnO}_3$ (LSMO) with thicknesses from 5 to 30 nm (see inset in Fig. 1). The magnetization vector of the $\text{La}_{0.7}\text{Sr}_{0.3}\text{MnO}_3$ epitaxial film lay in the plane of the substrate [21], whereas the magnetization vector of the SrRuO_3 film was usually directed at an angle of about 23° to the plane of the substrate [22]. The study of ferromagnetic resonance in the LSMO/SRO heterostructure at a frequency of 10 GHz showed the presence of uniaxial magnetic anisotropy characteristic of LSMO films [21]. However, the effect of the ferromagnetism of the SRO film was not revealed because of a high (about 1 T) saturation field of SRO. Peaks of three materials of heterostructures, YBCO, LSMO, and SRO, were observed in X-ray spectra of the LSMO/SRO/YBCO heterostructure. This indicates the epitaxial growth of films in the heterostructure and the absence of mixing of the materials at interfaces. The shape of the mesa-structure and feed lines for a direct current supply were formed using photolithography and plasmachemical and ion etching [16].

Parameters of the mesa-heterostructures at $T = 4.2$ K, where d_1 is the thickness of the SRO, d_2 is the thickness of the LSMO, L is the linear dimension of a mesa-heterostructure in the plane of the substrate, R_{NA} is the characteristic resistance of a mesa-heterostructure, $A = L^2$, and $j_C = I_C/A$ is the superconducting current density

The superconducting current was observed in all mesa-heterostructures with the total thickness d of the composite interlayer up to 53 nm, which is much larger than the coherence lengths of the ferromagnets of the interlayer ξ_F that are determined by the exchange field (see table).

To calculate the coherence length ξ_{LSMO} in the LSMO film, we used the exchange energy $E_{\text{ex}} = 2.3$ meV found from the measurements of the electron specific heat [23]. The estimate obtained in the dirty limit is $\xi_{\text{LSMO}} = 7$ nm at $v_F = 2 \times 10^7$ cm/s and the mean free path $l_{\text{LSMO}} = 0.4$ nm, which is calculated from the difference between the resistances of the autonomous LSMO film at room and helium temperatures [24]. The value $E_{\text{ex}} = 13$ meV for SRO was obtained from the measurements of the proximity effect at the SRO/YBCO interface [25]. In the dirty limit at $v_F = 10^7$ cm/s and the mean free path $l_{\text{SRO}} = 1$ nm, this gives the value $\xi_{\text{SRO}} = 2$ nm, close to the estimate obtained in [26]. The control measurements of the mesa-heterostructure with interlayer made only of LSMO [16] or only of SRO [27] showed that the critical current is absent for mesa-heterostructures where the SRO and LSMO spacers are thicker than 14 and 2 nm, respectively (see table).

The current density j_C of the mesa-heterostructures under study decreases by an order of magnitude with an increase in the total thickness of the spacer $d = d_1 + d_2$ from 8.5 to 53 nm. At the same time, a quite high value $j_C = 9$ A/cm² was observed for sample 930 ($d = 11.5$ nm, $L = 10$ μm , see table). The critical current density j_C depends nonmonotonically on the thickness d_2 of the LSMO (see Fig. 1). The low critical current density at small d_2 values (1.5 and 3 nm) is explained by the formation of the so-called dead (nonmagnetic)

| Sample | d_1 , nm | d_2 , nm | L , μm | R_{NA} , $\mu\Omega \text{ cm}^2$ | j_C , A/cm ² |
|--------|------------|------------|---------------------|-------------------------------------|---------------------------|
| 912 | 14 | 0 | 20 | 0.12 | 0 |
| 666 | 0 | 2 | 20 | 1200 | 0 |
| 932 | 5.5 | 3 | 30 | 0.11 | 2 |
| 930 | 5.5 | 6 | 20 | 0.15 | 9 |
| 978 | 4.5 | 3 | 50 | 0.45 | 0.75 |
| 934 | 23 | 30 | 30 | 350 | 0.3 |

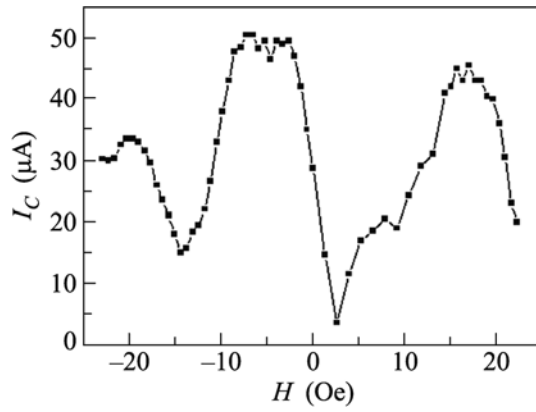


Fig. 2. Magnetic-field dependence of the critical current of the mesa-heterostructure with the dimensions $L = 50 \mu\text{m}$, $d_1 = 4.5 \text{ nm}$, and $d_2 = 3 \text{ nm}$ in the range of fields below the saturation field of the ferromagnetic interlayer at $T = 4.2 \text{ K}$.

layer at the interface, where ferromagnetic properties are suppressed with a decrease in the thickness of F. It can be seen that an increase in the total thickness of the interlayer d owing to the doubling of d_2 leads to a quadruple increase in the average j_C value for the sample with initially almost the same d_1 and d_2 values. It is noteworthy that the nonmonotonic dependence of the critical long-range triplet superconducting correlation on the thickness of one of the ferromagnets with the maximum at $d \approx \xi_F$ was theoretically predicted in [20], but for a more complex structure. A further significant increase in d in the experiment was accompanied by a decrease in the critical current according to the theoretical calculations reported in [17–20].

The measurements of the critical current I_C as a function of the magnetic field H (Fig. 2) show that it increases with the weak magnetic field from 5 to 15 Oe. The strength of the magnetic field at which the critical current is maximal depends on the parameters of the mesa-heterostructure and the direction of this field. Similar $I_C(H)$ dependences were observed for SFS junctions in which the long-range triplet superconducting correlation component of the superconducting current was induced [6, 11] as in the case of the ferromagnetic interlayer in SFS with the singlet component [28]. In the case of a wider variation range of the external magnetic field, hysteresis with a decrease in its amplitude is observed, indicating the existence of ferromagnetism in the spacer [28]. The $I_C(H)$ dependence shown in Fig. 2 does not exhibit hysteresis because the total range of variation of the magnetic field is much lower than the saturation magnetic field of the ferromagnetic layer [28].

The theoretical calculations reported in [17, 18] predict a strong increase (by several orders of magnitude) in the second harmonic of the phase dependence of the superconducting current $I_S(\varphi) = I_{C1}\sin(\varphi) + I_{C2}\sin(2\varphi)$ for the asymmetric interlayer ($d_1 \neq d_2$)

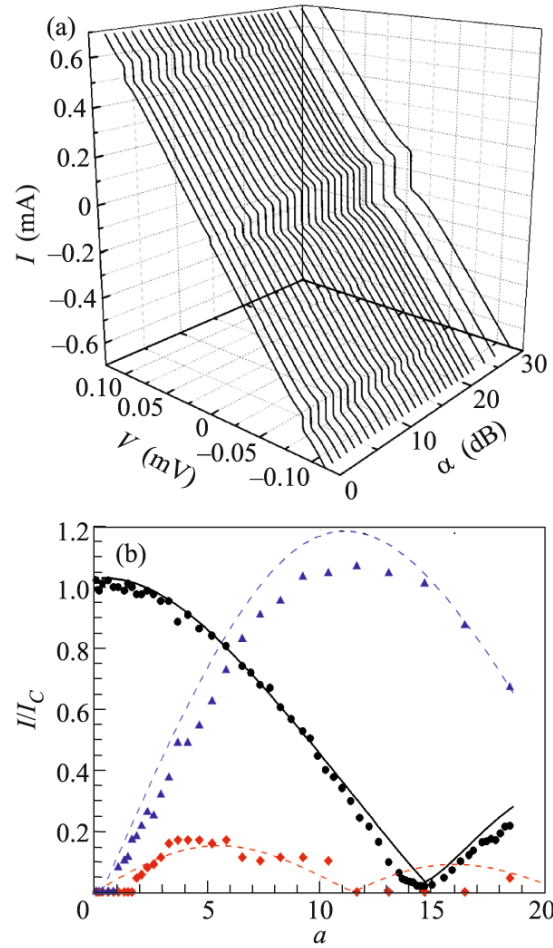


Fig. 3. Microwave properties of the mesa-heterostructure with $d_1 = 6 \text{ nm}$, $d_2 = 5.5 \text{ nm}$, and $L = 10 \mu\text{m}$ at $T = 4.2 \text{ K}$. (a) Family of the current–voltage characteristics of the mesa-heterostructure under microwave irradiation at a frequency of 41 GHz, where α is the damping constant (in decibels) owing to the external electrodynamic system. (b) (Circles) Critical current and amplitudes of the (triangles) first and (diamonds) half Shapiro steps versus the normalized amplitude of microwave radiation $a = I_{\text{RF}}/I_C$. The lines are the amplitudes with the second harmonic of the phase dependence of the superconducting current with $q = 0.13$ calculated within the modified RSJ model.

under the variation of the angle between the directions of the magnetizations of the F films, $I_{C2} \gg I_{C1}$. The measurements of the dynamics of variation of the Shapiro steps of the mesa-heterostructure demonstrate deviation from the sinusoidal current–phase relation. The current–voltage characteristics of the mesa-heterostructure with $L = 10 \mu\text{m}$, $I_C = 88 \mu\text{A}$, and normal resistance $R_N = 0.16 \Omega$ in the case of the action of monochromatic microwave radiation at a frequency of $f_e = 41 \text{ GHz}$ exhibit not only integer but also fractional Shapiro steps (Fig. 3a). For the critical frequency $f_C = (2e/h)I_C R_N = 6.8 \text{ GHz}$, the ratio $f_e/f_C = 6$ is in good agreement with RSJ model in the high-frequency limit. This is experimentally confirmed by the maxi-

mum of the first Shapiro step $I_1 = 94 \mu\text{A}$ and, correspondingly, by the ratio $I_1/I_C = 1.1$. In this case, the maximum height of the half-integer Shapiro step was $I_{1/2} = 15 \mu\text{A}$. Within the modified RSJ model [29] taking into account a nonsinusoidal current–phase relation, this value indicates that the fraction of the second harmonic $q = I_{C2}/I_{C1}$ is about 13%. It is worth noting that the direct comparison of the experiment with the theory developed in [17–19] is complicated because of the presence of the barrier between manganite and superconducting electrode. The authors of [20] stated that a long-range triplet superconducting correlations can hardly exist in the structure with two ferromagnetic layers. In our case, one of the S/M barriers is likely magnetically active and ensures the necessary function of the “third component.” It is not excluded that the antiferromagnetic layer appearing at the SRO/LSMO interface provides the function of the third component [30].

To summarize, we have experimentally detected the superconducting current in mesa-heterostructures with a composite bilayer oxide interlayer with noncollinear directions of the magnetizations in the layers. It has been shown that the total thickness of the interlayer is much longer than the length of ferromagnetic correlations, which is determined by the exchange field. The Josephson effect observed in these structures is explained by the penetration of the long-range triplet component of the superconducting order parameter into the magnetic interlayer. The deviation of the current–phase relation in the mesa-heterostructure from a sinusoidal dependence has been detected with a high fraction of the second harmonic; this deviation can also be due to the generation of the triplet component of the superconducting order parameter.

We are grateful to I. V. Borisenko, E. M. Goldobin, V. V. Demidov, A. V. Zaitsev, D. Winkler, A. S. Mel'nikov, T. Lofwander, and M. Fogelstrom for assistance in the experiment and stimulating discussions. This work was supported by the Division of Physical Sciences, Russian Academy of Sciences; the Ministry of Education and Science of the Russian Federation; the Council of the President of the Russian Federation for Support of Young Scientists and Leading Scientific Schools (project no. NSh-2456.2012.2); the Russian Foundation for Basic Research (project nos. 11-02-01234a and 12-07-31207mol_a); and the Swedish Institute (Visby program).

REFERENCES

1. F. S. Bergeret, A. F. Volkov, and K. B. Efetov, *Phys. Rev. Lett.* **86**, 4096 (2001).
2. F. S. Bergeret, A. F. Volkov, and K. B. Efetov, *Rev. Mod. Phys.* **77**, 1321 (2005).
3. V. L. Berezinskii, *JETP Lett.* **20**, 287 (1974).
4. A. I. Buzdin, *Rev. Mod. Phys.* **77**, 935 (2005).
5. I. Sosnin, H. Cho, V. T. Petrashov, et al., *Phys. Rev. Lett.* **96**, 157002 (2006).
6. R. S. Keizer, S. T. B. Goennenwein, T. M. Klapwijk, et al., *Nature (London)* **439**, 825 (2006).
7. M. S. Anwar, F. Czeschka, M. Hesselberth, et al., *Phys. Rev. B* **82**, 100501 (2010).
8. J. Wang, M. Singh, M. Tian, et al., *Nature Phys.* **6**, 389 (2010).
9. D. Sprungmann, K. Westerholt, H. Zabel, et al., *Phys. Rev. B* **82**, 060505(R) (2010).
10. J. W. A. Robinson, J. D. S. Witt, and M. G. Blamire, *Science* **329**, 59 (2010).
11. T. S. Khaire, M. A. Khasawneh, W. P. Pratt, et al., *Phys. Rev. Lett.* **104**, 137002 (2010).
12. P. V. Leksin, N. N. Garif'yanov, I. A. Garifullin, et al., *Phys. Rev. Lett.* **109**, 057005 (2012).
13. Y. Kalcheim, T. Kirzhner, G. Koren, and O. Millo, *Phys. Rev. B* **83**, 064510 (2011).
14. C. Visani, Z. Sefrioui, J. Tornos, et al., *Nature Phys.* **2318**, 1 (2012).
15. M. Van Zalk, A. Brinkman, J. Aarts, et al., *Phys. Rev. B* **82**, 134513 (2010).
16. A. M. Petrzhik, G. A. Ovsyannikov, A. V. Shadrin, et al., *J. Exp. Theor. Phys.* **112**, 1042 (2011).
17. L. Trifunovic, Z. Popovic, and Z. Radovic, *Phys. Rev. B* **84**, 064511 (2011).
18. A. S. Mel'nikov, A. V. Samokhvalov, S. M. Kuznetsova, et al., *Phys. Rev. Lett.* **109**, 237006 (2012).
19. I. B. Sperstad, J. Linder, and A. Sudbo, *Phys. Rev. B* **78**, 104509 (2008).
20. A. F. Volkov and K. B. Efetov, *Phys. Rev. B* **81**, 144522 (2010).
21. G. A. Ovsyannikov, A. M. Petrzhik, I. V. Borisenko, et al., *J. Exp. Theor. Phys.* **108**, 48 (2009).
22. G. Koster, L. Klein, W. Siemons, et al., *Rev. Mod. Phys.* **84**, 253 (2012).
23. B. F. Woodfield, M. L. Wilson, and J. M. Byers, *Phys. Rev. Lett.* **78**, 3201 (1997).
24. P. B. Allen, H. Berger, O. Chauvet, et al., *Phys. Rev. B* **53**, 8 (1996).
25. I. Asulin, O. Yuli, G. Koren, and O. Millo, *Phys. Rev. B* **79**, 174524 (2009).
26. L. Méchin, S. Flament, A. Perry, et al., *J. Appl. Phys.* **98**, 103902 (2005).
27. G. A. Ovsyannikov, A. E. Sheyerman, Y. V. Kislinskii, et al., in *Hybrid Superconducting Heterostructures with Magnetic Interlayer, Proceedings of the 19th Workshop on Oxide Electronics* (Apeldoorn, The Netherlands, 2012).
28. V. V. Bol'ginov, V. S. Stolyarov, D. S. Sobanin, et al., *JETP Lett.* **95**, 366 (2012).
29. P. Komissinskiy, G. A. Ovsyannikov, K. Y. Constantinian, et al., *Phys. Rev. B* **78**, 024501 (2008).
30. M. Ziese, I. Vrejoiu, E. Pippel, et al., *Phys. Rev. Lett.* **104**, 167203 (2010).

Translated by R. Tyapaev